

# AI-Based Stroke Rehabilitation Domiciliary Assessment System with ST-GCN Attention

Suhyeon Lim, Ye-eun Kim, and Andrew J. Choi.

**Abstract**—Effective stroke recovery requires continuous rehabilitation integrated with daily living. To support this need, we propose a home-based rehabilitation exercise and feedback system. The system consists of (1) hardware setup with RGB-D camera and wearable sensors to capture Stroke movements, (2) a mobile application for exercise guidance, and (3) an AI server for assessment and feedback. When Stroke user exercises following the application guidance, the system records skeleton sequences, which are then Assessed by the deep learning model, RAST-G@. The model employs a spatio-temporal graph convolutional network (ST-GCN) to extract skeletal features and integrates transformer-based temporal attention to figure out action quality. For system implementation, we constructed the NRC dataset, include 10 upper-limb activities of daily living (ADL) and 5 range-of-motion (ROM) collected from stroke and non-disabled participants, with Score annotations provided by licensed physiotherapists. Results on the KIMORE and NRC datasets show that RAST-G@ improves over baseline in terms of MAD, RMSE, and MAPE. Furthermore, the system provides user feedback that combines patient-centered assessment and monitoring. The results demonstrate that the proposed system offers a scalable approach for quantitative and consistent domiciliary rehabilitation assessment. Our code is available at <https://github.com/LimSuH/NRC-rehab>

**Index Terms**—AI, Attention, Deep Learning, Domestic, Recognition, Rehabilitation Assessment, Spatio-Temporal Graph Convolution Network, Stroke. Human action.

## I. INTRODUCTION

RECENT advancements in Neurology, particularly in motor control and learning, have revealed different mechanisms that induce changes in brain plasticity and behavior over both short- and long-term periods. Physical rehabilitation can be seen as a form of motor learning that occurs under specific conditions [1]–[4], and patients with motor impairments, such as those following a stroke, are capable of limited motor learning, although with variations in learning speed and volume. In particular, usage-based and reward-based learning, which are shaped by habitual, repetitive actions and rewards, play a key role in determining long-term brain and behavioral changes in stroke patients after they are discharged and resume daily activities. [5] Therefore, rehabilitation performed at domestic environments is significant in the patient’s recovery. However, without expert, improper rehabilitation can lead to injury and a professional training is essential for evaluations and feedback in order to provide effective rehabilitation. In this study, we propose AI-based Assessment model called RAST-G@ and a outline of rehabilitation monitoring system that can be used within the Domiciliary Environments. This system predicts the user’s rehabilitation movements RGB-D video data and expert assessment score collected during the system develop-

ment and experiment. Many existing studies provide limited evaluation for topical motion segments. (ex: Range of Angle) But ours takes the sequence of actions as input and learns it with a Spatio-temporal graph based deep learning method (GCN). Since movements are continuous inputs Through time, temporal feature learning is important to evaluate the quality of actions. We enhanced temporal learning results by introducing Temporal Attention, which has proven the performance in deep learning. evaluation Questionnaires from professional therapists contain the quality of complex actions. RAST-G@, the model that end-to-end deep learning-based rehabilitation Assessment is able to assist healthcare providers and contributes to quantitative and consistent assessments of rehabilitation without the need for separate standardization processes. In this paper, We propose an end-to-end deep learning-based rehabilitation Assessment model. This model assists healthcare providers and contributes to quantitative and consistent assessments of rehabilitation without the need for separate standardization processes. It has the potential to enhance the activation of the rehabilitation and the quality of healthcare.

## II. RELATED WORKS

Deep learning has applicated in rehabilitation research, as these methods enable the automated processing of complex motion data and biosignals, thereby reducing the subjectivity inherent in conventional clinical assessments and allowing for more precise and objective measurements. The integration of deep learning is expected to enhance therapeutic efficiency, support the development of personalized rehabilitation strategies, and facilitate continuous monitoring of functional recovery. Within this context, two primary types of tasks are generally distinguished: *Recognition and Assessment*.

### A. Human Action Representation

One of the most important factors in a deep learning-based framework is the dataset. The higher quality human behavioral representations within dataset, the more meaningful features can be extracted. However, human behavior is abstract high-level data that is in multiple dimensions. Consequently, extensive research has been devoted to identifying the most suitable representation. Traditionally human action representations have been sensor-based. [6], [7] Sensor-based studies have been widely conducted in the rehabilitations. For example, M. Panwar et al., [8], attached 3-axis accelerometers to classify arm movements including Reach and retrieving, lifting and Rotating arm. in stroke rehabilitation. Similarly, B. Pogorelc

et al., [9] recognized gait patterns of elderly to enable early detection of health problems. Sensor data are advantageous in rehabilitation contexts where continuous monitoring is required, offering benefits in the cost and robustness against environments compared to RGB vision data. On the other hand, vision-based modalities, while computationally heavier and susceptible to privacy concerns and background noise, have gained attention for their convenience in capturing full-body motion. [10] Sensors are dependent on placement and attachment, and reconstructing full-body correlation structures often requires additional procedures. In contrast, vision-based approaches impose less burden on participants and allow for easier equipment installation. To overcome the limitations of both approaches, recent deep learning Method has adopted more processed representations, particularly skeleton-based data [7], [11]. Skeleton represents the human body as a set of landmarks corresponding to joints connected according to anatomical structure. This representation facilitates the modeling of joint interactions through graph, mitigates weaknesses of vision, such as sensitivity to background noises [12], and occlusion and depth ambiguities can be compensated.

### B. Recognition and Assessment

Recognition tasks are designed to categorize input data, ordinarily sequential Data, into predefined discrete labels. Within the broader domain of human action recognition, these tasks aim to identify and differentiate human actions from motion or sensor-derived signals. Unlike simple classification, however, recognition addresses continuous data that may contain inseparable or irrelevant segments. Many studies have extended deep learning networks designed for recognition tasks. A example is the Spatio-Temporal Graph Convolutional Network (ST-GCN) [13], which has proven particularly effective for skeleton. In skeleton graphs, joints are represented as nodes and anatomical connections as edges, enabling effective modeling of human actions. Since human action is characterized by the coordinated movements of multiple joints, ST-GCNs are good for capturing their relational dependencies. Building upon spatio-temporal skeleton recognition [14], demonstrated that even simple data augmentation techniques can yield state-of-the-art performance. Duan et al., [15] proposed a model that transforms skeletons into heatmaps and trains them using 3D Convolutional Networks. This approach mitigates the impact of outliers arising from pose estimation errors, thereby achieving strong performance in action recognition. When applied to rehabilitation, recognition focuses on categorizing rehabilitation-specific movements. This constitutes a high-dimensional and comprehensive task; as atypical data, it involves not only the identification and segmentation of meaningful rehabilitation-related behaviors from patients' irregular movements but also their transformation into clinically interpretable information. Assessment is related to recognition, as high-quality evaluation requires clear distinction and the meaningful features. In rehabilitation, assessment tasks aim to measure the quality of movement. Prior implementations have attempted to map performed movements to corresponding quality scores. However, a major challenge in this domain is

that rehabilitation assessment metrics are subjective and may significantly depending on the evaluation tool employed. With this issue, earlier research used distance Metrics to produce quantitative assessments. Examples include methods based on Mahalanobis distance [16] and Dynamic Time Warping (DTW) algorithms [17]–[20] which measure the distance between a reference movement and a patient's movement. While these approaches provide objective values, they are sensitive to noise and lack sufficient verification as reliable rehabilitation metrics. M. Capecci et al., [21] demonstrated that DTW assessments deviate from clinical assessment, highlighting the importance of temporal dynamics in the assessment process. Other attempts include mapping handcrafted features to clinical scores [22] though such approaches require multiple models and incur additional computational cost. The Fugl-Meyer Assessment (FMA) is also widely used as a quantitative clinical Metric. However, its scoring system –{0: The patient cannot perform the task, 1: The patient performs the task partially, 2: The patient fully performs the task.} –is limited in granularity, potentially making item descriptions overly complex and less adaptable for automated assessment.

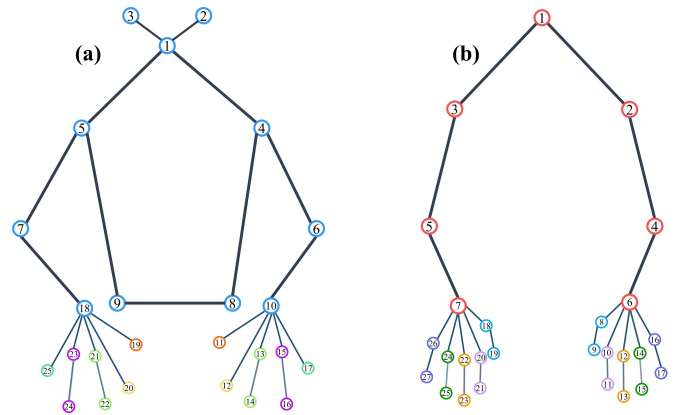


Fig. 1. Upper limb skeleton keypoints used in this Study. (a) Basic 25 configuration, (b) Additional 27 configurations.

### C. Deep Learning Network for Human Action

Traditionally, human action data have been modeled in deep learning frameworks using a combine of spatial (skeleton-based) and temporal networks. The temporal dimension is particularly critical, as the sequential nature of movements often has a more direct impact on model performance than static body configurations. Liao et al., [23] simultaneously incorporates spatial structure and temporal dynamics. Their method progressively learned five human body subsets and integrated them to capture overall motion, ensuring that temporal dependencies were reflected in the model. Because of limited rehabilitation datasets, they also employed a temporal pyramid structure that subsampled motion sequences. However, the convolutional networks used for spatial learning were not well suited for skeleton data, where body joints are deeply interrelated. [24] This limitation naturally motivated the adoption of Graph Convolutional Networks (GCNs), which can preserve connectivity of the human body. [25] Deb et

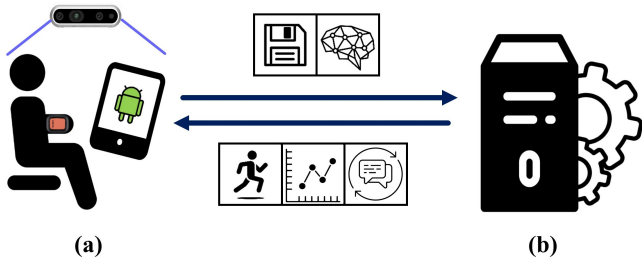


Fig. 2. Overall System architecture. (a) Hardware setup and rehabilitation exercise interface using the proposed system (RGB-D camera, IMU, and android os mobile device), (b) Server component for storing collected data, running model inference, and managing feedback transmission.

TABLE I  
NRC DATASET OVERALL

Subject	Train	Validation	Test	Total
ND	293	32	-	325
Stroke	633	70	114	817
Total	916	112	114	1,142

al., [26] presented a notable example introducing GCNs into rehabilitation. Learning sequential data into a Spatio-Temporal GCN (ST-GCN), A single model could evaluate multiple types of movements. From prior works, their also incorporated Long Short-Term Memory (LSTM) networks for temporal modeling, inspired by Liao et al. As a variant of recurrent neural networks (RNNs), it designed for the vanishing gradient and long-term memory problems by gating mechanisms. Nonetheless, LSTMs still suffer from limitations in modeling very long-term dependencies [27] and their complexity leads to overfitting and interpretability issues. [28]

### III. METHODS

the objective of this study is to learn a regression function  $f_{\theta} : X \rightarrow Y$  that maps an input motion sequence  $X \in \mathbb{R}^{N \times C \times T \times V \times M}$  to a continuous assessment score  $Y$ , as provided by clinical experts. Here,  $N$  is the batch size,  $C$  is the channel dimension,  $T$  is the sequence length,  $V$  is the number of keypoints (25 joints in Fig. 1(a)), and  $M$  is the number of instances. The output  $Y$  is a scalar score annotated by clinicians for both stroke patients and non-disabled participants. Based on this formulation, we describe the acquisition of clinically relevant rehabilitation data and the design of assessment items, and the proposed network that combines ST-GCN and Transformer-based attention modules to effectively capture the spatio-temporal characteristics of skeleton sequences.

#### A. Collecting Dataset

Domiciliary rehabilitation systems demand both efficiency and intuitive usability. To achieve this, we designed the system pipeline such that each module operates in coordination. Because rehabilitation data for stroke patients is costly and difficult to acquire, whenever a user performs rehabilitation exercises, the software simultaneously conducts recognition and assessment while recording data for training. The overall

TABLE II  
15 ACTION CLASSES WITH 10 ADL, 5 ROM

#	Class	Description	Cate.	Tool
1	LiftCupHandle	Drinking water with a cup	UNI	Cup
2	HairBrush	Brushing hair	UNI	Comb
3	BrushTeeth	Brushing teeth	UNI	Toothbrush
4	Remotecon	Remote controller	UNI	Controller
5	MovingCan	Moving a tool	UNI	Can
6	Writing	Writing with one hand while holding paper with the other	BIA	Pencil
7	FoldingPaper	Folding paper	BIA	Paper
8	FoldupTowel	Folding towel	BIA	Towel
9	WashFace	Washing face	BIS	-
10	Smartphone	Using cellphone	BIS	Cellphone
11	RightShoulderFrontal	flexion the right arm	BIA	-
12	LeftShoulderFrontal	flexion the left arm	BIA	-
13	RightShoulderSide	abduction the right arm	BIA	-
14	LeftShoulderSide	abduction the left arm	BIA	-
15	LateralRotation	shoulder external rotation	BIS	-

system is illustrated in Fig. 2. The hardware setup includes a mobile tablet, an RGB-D camera, and IMU sensors. The software provides exercise guidance, records the corresponding data, and presents evaluation results. The recording function manages exercise execution and data collecting, while the assessment function connects with the server to present assessment score.

1) **Rehabilitation Actions Data:** Using The proposed system, We collected a multimodal rehabilitation dataset. The hardware setup included an Intel RealSense D435i depth camera and Movella Xsens Dot sensors. From these, RGB-D videos were captured, and acceleration-Gyroscope  $(x, y, z)$  was collected from attached devices to both wrists. For the Assessment model presented in this paper, only RGB-D data was used, in order to maintain compactness and interpretability. The Classes consisted of 15 movements in Table. I. Including both Activities of Daily Living (ADL) and Range of Motion (ROM) tasks, chosen to evaluate upper-limb functional ability. [29] The movement set was confirmed under consultation with faculty members in physical therapy. As in Table. II., data was collected from two participant groups: non-disabled (ND) and stroke patients. Skeleton keypoints were estimated from the Captured RGB-D videos. We adopted 25 keypoints configuration, which is the most widely used representation in skeleton-based human motion analysis. This ensures compatibility with existing skeleton-based benchmarks such as OpenPose [30] and COCO WholeBody [31], both of which are based on 25 full-body keypoints. Since many prior works have leveraged these benchmarks for human motion analysis, the 25 keypoints not only enables performance comparison but also aligns with well-studied graph construction methods. This experiment for collecting dataset was pproved by the IRB of Gachon university before proceeding (IRB no. 1044396-202306-HR-102-02)

2) **Assessment Score:** The most significant component of the assessment dataset was evaluation items. As noted in prior studies [17]–[22] and in the representative rehabilitation

TABLE III  
REHABILITATION EXERCISE ASSESSMENT QUESTIONNAIRES ARE  
SCORED ON 0-5 LIKERT SCALE.

#	Questionnaire
1	Are the main objectives of the action achieved?
2	Is the body moved without instability during the action?
3	Is the action performed smoothly and continuously without interruption?
4	Is the head movement performed correctly?
5	Is the right arm performed correctly?
6	Is the left arm performed correctly?
7	Is the trunk performed correctly?
8	Is the task performed without dropping or missing the tool in the hand?
9	Are the force, speed, and direction appropriately controlled during the action?
10	Is the action trajectory self-regulated during motion?

dataset UI-PRMD [32], Most existing approaches reference the movements of ND as ideal motions. However, according to Birke et al., [33], The main goal of neurological rehabilitation is the improvement of function and independence. In other words, rehabilitation assessment focuses on achieving functional activities and participation [34], rather than the mere removal of impairments. Consequently, the quality of a top grades movement performed by a Stroke cannot be equated with that of a ND. This underscores the need for stroke-centered Assessment criteria. Although detailed clinical assessments can be applied, subjectivity remains a concern. Therefore, there is a need to establish new set of evaluation items with upper-limb rehabilitation tasks. The KIMORE [35] provides an illustrative example of balancing quantitative and clinical evaluation: it employs 10 items, each scored on a 5-point Likert scale, resulting in a maximum score of 50 per trial. Table. II. summarizes the questionnaire items used in NRC(ours). We developed evaluation items specifically designed for the 15 upper-limb movements. The items were initially drafted through discussions among three licensed physiotherapists with more than five years of clinical experience, and validated by two Ph.D. members in physical therapy. Item 2 and 3 were under the assumption that each movement is performed only once, while 8,9 and 10 address seated tasks involving upper-limb usage. In particular, item 8 evaluates fine motor skills such as handling small objects, which are essential for assessing activities of daily living (ADL).

### B. Model Structure

As reported by Deb et al., [26], Graph Convolutional Networks (GCNs) are effective as a framework for assessing rehabilitation movements. Human motion can be represented as a graph, with skeleton keypoints as nodes and anatomical connections as edges. However, this corresponds only to the spatial representation of the human skeleton. human movements are expressed as sequential information, a temporal dimension is required in the network. For this reason, spatio-temporal GCNs (ST-GCNs) have been shown to be effective in human action deep learning tasks [13]. Rehabilitation movement assessment can be regarded as a

subtask of human action and thus inherits these properties; in our methods, through skeleton-based ST-GCN, spatial skeleton information is connected along the temporal dimension. The model structure is illustrated in Fig. 3. The skeleton consists of 25 keypoints, including the upper limbs and both hands. The first ST-GCN block takes as input the skeleton coordinates  $X \in \mathbb{R}^{N \times C \times T \times V \times M}$  and the graph  $G = (V, E, A)$  where adjacency matrix is  $A \in \mathbb{R}^{K \times V \times V}$ , where  $C$  denotes the channel dimension,  $T$  the frame-sequence length, and  $V$  the number of keypoints. The skeleton graph is constructed for each frame from human joint coordinates, and convolution is performed across both spatial and temporal dimensions. For hop distance  $k$ , the adjacency matrix  $A$  is normalized as  $\tilde{A}_k^{(l)} = D_k^{-1/2} (A_k \odot E_k^{(l)} + I) D_k^{-1/2}$ . At the  $l$ th layer, each ST-GCN unit is defined as in (1) and (2). Equation (3) representates an ST-GCN Block.

$$S_l(X) = \sigma \left( \sum_{k=1}^K \tilde{A}_k X W_k^{(l)} \right) \quad (1)$$

$$\Gamma_l(X) = \sum_{c=1}^C \sum_{\tau=-\lfloor k_t/2 \rfloor}^{\lfloor k_t/2 \rfloor} U_{C,c,\tau}^{(l)} Z_{n,c,t+s_t\tau,v} + b_C^{(l)} \quad (2)$$

$$X_l = \sigma(\Gamma_l(S_l(X_{(l-1)})) + r_l(X_{(l-1)})) \quad (3)$$

Fig. 3(c) illustrates a single ST-GCN unit. All units, except for the first, operate with residual structure. After each convolution along the spatial and temporal axes, Batch Normalization and ReLU activation are applied. the output is concatenated with the initial input to preserve the original information. While ST-GCN is powerful in extracting local and sequential patterns, it has the limitation that all joints and temporal segments are treated with equal weight. In actual human actions or rehabilitation movements, certain joints (e.g., wrist, shoulder) or time points (e.g., the beginning or end of a movement) are often more important. Transformer has demonstrated the effectiveness of self-attention mechanisms in deep learning [36]. We adopt Transformer-based network within RAST-G@ to enable score assessment as illustrated in Fig. 3(d). Multi-head attention is applied across the temporal axis for each joint. This still allows temporal features to be learned, but unlike LSTM-based models that aggregate global temporal information across joints, it performs joint-specific temporal attention. Since this does not require additional adjacency matrix operations, it reduces computational overhead while remaining effective for long-term memory. To perform attention along the temporal axis, the Temporal Attention;(TA) module reshapes the input  $X$  to  $X' \in \mathbb{R}^{(N \times V) \times T \times C}$  For head  $h$ , the query, key, and value matrices are computed as  $Q_h = X' W_h^Q$ ,  $K_h = X' W_h^K$ , and  $V_h = X' W_h^V$ . The output is computed as a weighted sum of the values, where the weight assigned to each value is computed by a compatibility function of the query with the corresponding key. The input consists of queries and keys of dimension  $d_k$ , and values of dimension  $d_v$ . Then Compute the dot products of the query with all keys, divide each by  $\sqrt{d_k}$  and apply a softmax function to obtain the weights on the values. [37]

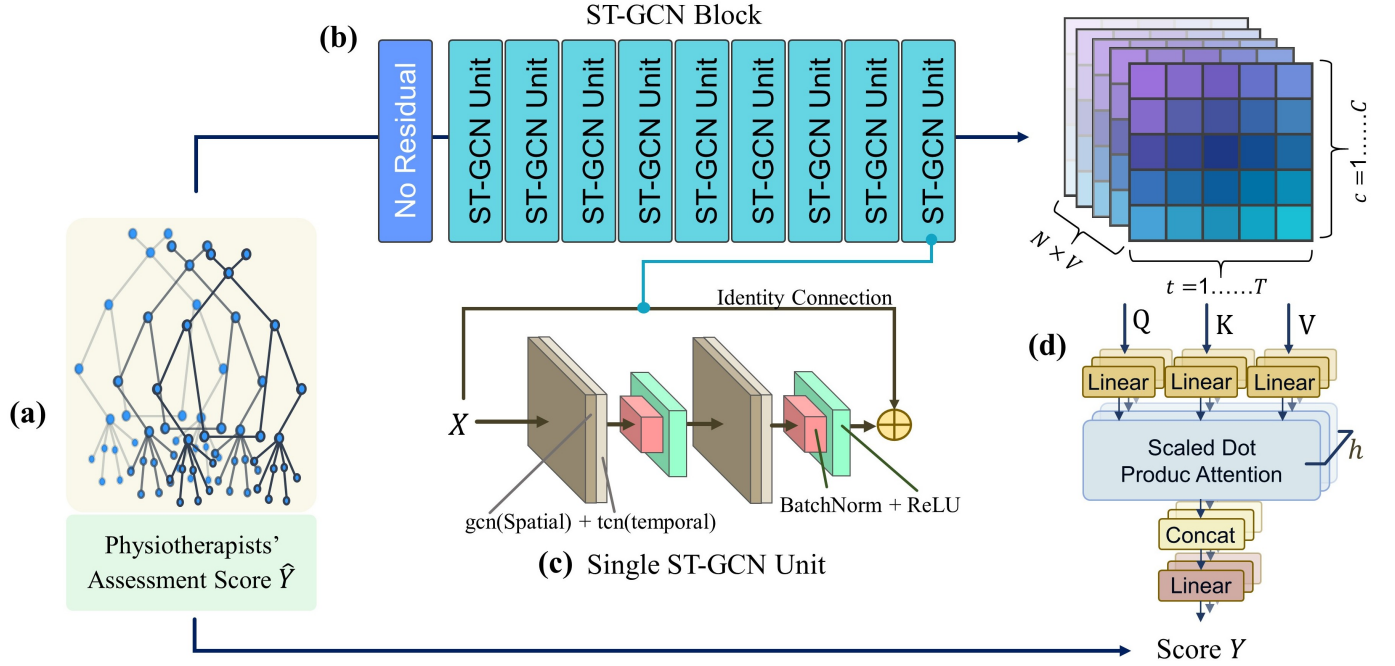


Fig. 3. Overview of RAST-G@ Model Structure. (a) Skeleton sequence and Score input, (b) Outputs 3d feature map  $X' \in \mathbb{R}^{(N \times V) \times T \times C}$  via STGCN Block from skeleton spatio-temporal graph. (c) Structure of a single ST-GCN unit. After GCN and TCN layers, followed by Batch Normalization and ReLU; the output is concatenated with the initial input through residual connections. (c) Transformer attention block. From the ST-GCN output, the query (Q), key (K), and value (V) are obtained, and the attention scores are computed as in (4). (d) The prediction  $Y$  is compared with the ground-truth scores,  $\hat{Y}$

$$Y = W_2 \sigma(W_1 z + b_1) + b_2 \quad (4)$$

After learning the attention weights for all sequences, the model outputs a single scalar score representing the quality of the movement. regression head is employed to predict scores over a wide range and diverse cases. The regression module consists of an average pooling layer followed by a linear layer. Pooling aggregates spatio-temporal features into a compact representation  $z' \in \mathbb{R}^{N \times C \times 1 \times 2}$ , and the linear layer gets this feature to a scalar score  $Y$ , in (4). The final model output  $Y$  is compared with the ground-truth scores assigned by expert physiotherapists. For model optimization, the *Huber Loss*, (5) is used with  $\delta=0.1$  allowing a selective application of MSE and MAE. When the error is below MSE emphasizes sensitivity to small deviations, while for errors exceeding MAE mitigates the influence of outliers.

$$L_\delta(y, \hat{y}) = \begin{cases} \text{MSE}(y - \hat{y}), & |y - \hat{y}| \leq \delta \\ \delta \text{MAE}(y - \hat{y}) - \frac{\delta^2}{2}, & |y - \hat{y}| > \delta \end{cases} \quad (5)$$

#### IV. EXPERIMENT

##### A. Setup

1) **Dataset:** We conduct experiments on data scored on a 50-point scale based on the Likert method. The datasets include both whole-body and upper-body rehabilitation exercises. whole-body tasks reflect global motor coordination, while upper-body tasks emphasize fine motor control of the arms and hands. conducting experiments on the two datasets, we evaluate the model performance in assessing different

rehabilitation exercises. **a) KIMORE** Kinematic assessment of Movement for remote monitoring of physical Rehabilitation, called KIMORE [35] is a dataset consisting RGB-D videos and score annotations for five whole-body exercises. The Subject groups(GPP) are divided according to the presence or absence of pain or disability. The non-pain group(CG) includes motions performed by 12 professionals include physiotherapist, as well as 32 non-professionals. The GPP group consists of 34 subjects with conditions such as Parkinson's disease, back pain, and stroke. Score annotations for each exercise were provided by a professional rehabilitation therapist. **b) NRC(ours)** This dataset consists of upper-limb rehabilitation movement data collected using RGB-D cameras, IMU sensors, and dedicated software. It includes 15 exercises comprising 10 activities of daily living (ADL) and 5 range of motion (ROM) tasks in Table. I . The ADL set emphasizes upper-body and finger movements relevant to daily life. We further categorized the exercises into three groups: UNI (Unimodal Hand Using), BIA (Bimodal and Asymmetric Hand Using), and BIS (Bimodal and Symmetric Hand Using). These categories enable comparative analysis of the model performance in assessment score mappings across different types of movements. All motion data include score annotations provided by professional rehabilitation therapists. For this purpose, we developed a new set of 10 dedicated evaluation items.

We designed an end-to-end system for rehabilitation recognition and assessment using deep learning, with the proposed model corresponding to the rehabilitation assessment module. For this task, the model was trained on data from six non-disabled (ND) subjects and eleven stroke patients. The effectiveness of rehabilitation depends on the time of onset

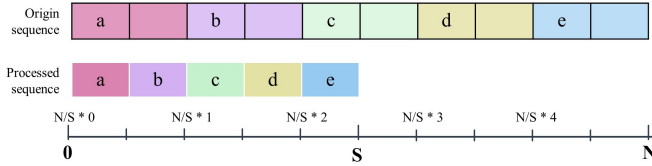


Fig. 4. Uniform Frame Sequence Method.

[38]. This factor represents a main requirement for the goal of our system, which is to enable patients to perform rehabilitation exercises independently at home. Accordingly, patient recruitment focused primarily on subacute stroke patients with hemiplegia within six months of onset. The detailed conditions for the recruited stroke participants are as follows:

- Age 19 years or older
- Subacute or chronic stage
- Upper-Limb hemiplegia
  - FMA  $\geq 30$
  - Brunnstrom’s stage hand recovery 4-4.5 stage
- Understand and communicate about the experiment
  - MOCA  $\geq 22$

In total, 1,142 movement–score pairs were used, segmented by exercise. The dataset was split into train, validation and test sets at approximately 8:1:1 ratio. A summary of the datasets is provided in Table I.

2) **Preprocessing:** **a) Pose estimation** The raw data consists of RGB-D video sequences, which requires an additional step of skeleton keypoint estimation. For this purpose, we employed MMPose [39], an open-source human pose estimation library developed by the OpenMMLab team. This framework provides a unified interface for researchers and developers to train, infer, and evaluate a wide variety of pose estimation models. In our work, we performed inference using the HRNet-DarkPose model [40], [41], which was trained on the COCO-WholeBody dataset [31], to estimate human poses. The extracted skeleton structure is presented in Fig. 1. **b) Uniform Frame Sequences** Standardizing frame sequences into a uniform format is a critical preprocessing step for deep learning models. Although individual actions may differ in temporal characteristics (e.g., length, speed), consistency across the dataset is required. Inevitably, this process involves partial loss of motion information. To mitigate this, we applied a frame drop preprocessing strategy. As illustrated in Fig. 4., the original sequence was divided into groups at intervals of  $N$  frames, and a frame was sampled from each group and concatenated sequentially. This approach preserves the original temporal tendency. It also allows frame shifting for random sampling within groups, which enhances data variability and supports augmentation. Using this method, all sequences were standardized to a length of 288 frames.

## B. Training

The implementation and training were conducted on an Intel i9-10920X CPU and an NVIDIA GeForce RTX 4090 GPU. All model frameworks were implemented in PyTorch

on Ubuntu 22.04.05 LTS. The hyperparameters were set as follows: 200 epochs, batch size of 64, and AdamW optimizer with a learning rate of 0.003. For performance evaluation, Mean Absolute Devian (MAD), Root Mean Square Error (RMSE), and Mean Absolute Percentage Error (MAPE) were employed. These metrics quantify the discrepancy between ground truth and model predictions in terms of mean, root square, and percentage error, respectively. The equations are as follows:

$$\text{MAD} = \frac{1}{n} \sum_{i=1}^n |y_i - \hat{y}_i| \quad (6)$$

$$\text{RMSE} = \sqrt{\frac{1}{n} \sum_{i=1}^n (y_i - \hat{y}_i)^2} \quad (7)$$

$$\text{MAPE} = \frac{1}{n} \sum_{i=1}^n \left| \frac{y_i - \hat{y}_i}{y_i} \right| \times 100 \quad (8)$$

## V. RESULT

### A. Overview

We carefully distinguished between baseline models in our paper. Deep learning research for rehabilitation assessment remains a task with significant potential, yet reliable prior studies are still restrictive. Accordingly, we employed existing human-task deep learning models for performance comparison. The models listed in Table IV under the Recognition Model–FC layer category correspond to this approach. References [13], [43]–[46] were designed for recognition tasks. For assessment, their last softmax layers were replaced with fully connected layers. This is possible since both assessment and recognition rely on extracting qualitative information from human action data. Since human behavior is a high-level construct involving multiple modalities, several studies have explored multimodal deep learning rather than relying on a single modality. Kuang et al. proposed a hierarchical approach that separately learned position and orientation and then integrated them for joint representation.

1) **KIMORE Dataset Result:** we compared RAST-G@ with baseline models using three metrics, (6), (7), (8). The results in Table IV, The model improved accuracy and maintained consistent performance across all five actions, indicating the model’s potential applicability not only to full-body tasks but also to diverse rehabilitation movements and assessment domains. Among the three evaluation metrics, MAD showed modest improvement over previous models, whereas RMSE and MAPE demonstrated substantially larger gains. This is because of the metric definitions. MAD averages absolute errors and is less sensitive to large deviations, whereas RMSE and MAPE capture the influence of large errors and their proportion relative to overall predictions.

The results of Ex4 also provide an important indicator. Relative Works have reported particularly low errors for this action, which can be explained by its nature. This Exercise is pelvis rotations on the transverse plane while keeping other body parts fixed, where rotational variation provides better representation than translational displacement. In a Cartesian

TABLE IV  
COMPARISON OF ASSESSMENT DEEP LEARNING MODEL RESULTS ON KIMORE USING RMS, MAPE AND MAD METRICS (LOWER VALUES INDICATE BETTER PERFORMNACE)

Metric	Ex	Assessment				Recognition + FC Layer				
		RAST-G@ (ours)	Kuang <i>et al.</i> [42]	Deb <i>et al.</i> [26]	Liao <i>et al.</i> [23]	Zhang <i>et al.</i> [18]	Song <i>et al.</i> [43]	Yan <i>et al.</i> [13]	Li <i>et al.</i> [44]	Du <i>et al.</i> [13]
RMSE ↓	Ex1	<b>0.267</b>	0.399	2.024	2.534	2.916	2.165	2.017	2.344	2.440
	Ex2	<b>0.268</b>	0.354	2.120	3.738	4.140	3.345	3.262	2.823	4.297
	Ex3	<b>0.274</b>	0.289	0.556	1.561	2.615	1.929	0.799	2.004	1.925
	Ex4	0.264	<b>0.101</b>	0.644	0.792	1.836	2.018	1.331	1.078	1.676
	Ex5	<b>0.264</b>	0.386	1.181	1.914	2.916	3.198	1.951	2.575	3.158
	AVG	<b>0.267</b>	0.306	1.305	2.108	2.8846	2.531	1.872	2.165	2.699
MAPE ↓	Ex1	<b>0.364</b>	0.431	1.926	2.589	5.054	2.605	2.339	3.491	3.228
	Ex2	<b>0.370</b>	0.749	1.272	3.976	10.436	3.296	6.136	5.298	6.001
	Ex3	0.385	<b>0.271</b>	0.728	2.023	5.774	2.968	1.727	4.188	3.421
	Ex4	0.346	<b>0.173</b>	0.824	2.333	3.901	2.152	2.325	1.976	2.584
	Ex5	<b>0.349</b>	0.692	1.591	2.312	6.531	4.959	3.802	5.752	5.620
	AVG	<b>0.363</b>	0.463	1.268	2.647	6.3392	3.196	3.266	4.141	4.171
MAD ↓	Ex1	0.225	<b>0.186</b>	0.799	1.141	1.757	0.977	0.889	1.378	1.271
	Ex2	<b>0.227</b>	0.235	0.774	1.528	3.139	1.282	2.096	1.877	2.199
	Ex3	0.231	<b>0.111</b>	0.369	0.845	1.737	1.105	0.604	1.452	1.123
	Ex4	0.221	<b>0.053</b>	0.347	0.468	1.202	0.715	0.842	0.675	0.880
	Ex5	<b>0.220</b>	0.223	0.621	0.947	1.853	1.536	1.218	1.662	1.864
	AVG	0.225	<b>0.162</b>	0.582	0.986	1.938	1.123	1.130	1.409	1.467

representation, depth (z-axis) serves as the primary feature, whereas in a quaternion representation, the motion can be more effectively expressed through roll and pitch axes. Thus, the method of Kuang *et al.* was well suited for this action, showed very small errors.

These result finds that our model is not specialized for a single action but instead maintains robust performance across a diverse set of movements. Its stability becomes more pronounced as the number of predicted actions increases and as inter-action variability grows. Consequently, RAST-G@ is advantageous for stroke rehabilitation assessment, where patient-specific movements differ and long-term monitoring is required.

TABLE V  
COMPARISON OF ASSESSMENT DEEP LEARNING MODEL RESULTS ON NRC DATASET(OURS)

Metric	RAST-G@	Kuang <i>et al.</i>	Deb <i>et al.</i>
RMSE ↓	<b>0.291</b>	1.961	1.030
MAPE ↓	<b>0.259</b>	2.836	3.805
MAD ↓	<b>0.321</b>	0.739	0.892

2) *NRC(Ours) Dataset Result*: The NRC dataset collected for this study includes activities of daily living (ADL) and range of motion (ROM) exercises. ADL tasks consist of relatively dense and complex movements and are generally more difficult compared to other actions. They are further constrained to the upper extremities, concentrating motion information in the arms and fingers. For baseline, we compared our method with graph-based deep learning approaches proposed by Kuang *et al.*, [42] and Deb *et al.*, [26]. Kuang *et al.* employed a hierarchical strategy that separately learned

position and orientation, later integrating the two for joint representation. Orientation was represented by four-dimensional quaternions  $(x, y, z, w)$  which show the directional state of each joint [47]. Accordingly, it was necessary to generate appropriate orientation data from the NRC dataset prior to experimentation. Algorithm 1. describes this procedure. Given  $J$  skeletons, a skeleton sequence  $seq$ , and an edge tuple array  $E$ , the function BUILD\_PARENTS takes  $J$  and  $E$  as input and returns an index array  $P$  indicating the parent joint of each joint  $j$ . The function QUATERNION\_SEQUENCE then takes  $seq$ ,  $P$ , and the previous skeleton frame  $prev$  from,  $i - 1$  as input, and returns a sequence of joint-wise quaternions. A reference REST pose is computed to serve as the baseline for rotation estimation. For each joint  $j$  the parent-child connection is used to calculate the rotation from the baseline pose. A reference vector  $up_0$  is introduced for computing the roll angle around the  $y$ -axis, ensuring orthogonality of the  $x, y, z$  rotation axes. This process is repeated for each frame  $T$  producing quaternion sequences. Finally, the angular differences between the reference pose and the current pose are computed to form matrices  $D_{t,j}$ , which are transformed into  $Q \in \mathbb{R}^{T \times J \times 4}$ .

When trained on the NRC dataset with both position and orientation features, RAST-G@ achieved substantial improvements over baseline models. This result means the characteristics of the NRC dataset, unlike repetitive tasks, includes goal-directed movements accompanied by fine finger control. Emphasizing temporal modeling led to superior performance, as summarized in Table. V. Whereas other baseline models exhibited error increases of up to fivefold when transferred to the NRC dataset, RAST-G@ maintained stable accuracy, thereby demonstrating robustness. Moreover, the model con-

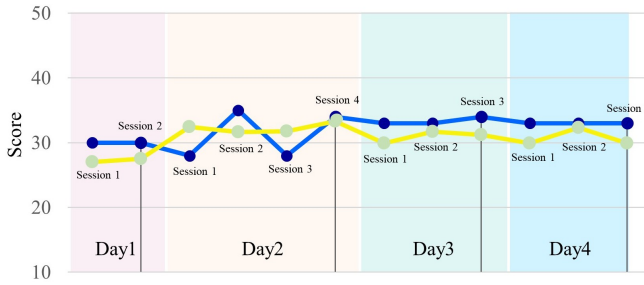


Fig. 5. Visualization of NRC works(yellow) compare to therapists’ score(blue) during 4 month long-term dataset. label02: brushing hair, Stroke 14.

TABLE VI  
METHOD ABLATION STUDY RESULT

Method	MAD ↓	RMSE ↓	MAPE ↓
frame Drop	0.260	0.326	0.379
Temporal Attention	0.277	0.340	0.480
Stroke Only	0.250	0.303	0.335
Proposal	0.259	0.321	0.291

sistently outperformed baselines in error measures that account for outliers (e.g., RMSE) and relative error magnitude (e.g., MAPE). Notably, MAPE even decreased further, underscoring the model’s potential for rehabilitation domains characterized by high input variability.

Fig. 5. presents the ground-truth scores provided by therapists and the predictions of RAST-G@ about NRC dataset. A longitudinal study was conducted once per month over four months, during which action data and therapist scores for our assessment were collected. The comparison shows that the model not only learned the overall trend of score but also provided good quality score predictions.

### B. Ablation Study

In Table. VI., The frame dimension is a critical factor for representing action sequences, and the strategy used to construct uniform input sequences directly affects the model’s perception of motion. Frame dropping, which reduces sequence length while preserving the overall temporal flow, is one of the core components of RAST-G@. Without frame dropping, the model yielded the lowest MAPE, although MAD and RMSE did not differ substantially from the proposed method. This indicates that preprocessing without considering full action sequences can distort temporal information and result in larger relative errors.

The temporal Attention aimed to learn fine-grained rehabilitation movements by leveraging a deeper neural network architecture. without the method showed the most significant performance degradation, underscoring the importance of temporal information for aligning rehabilitation motions with qualitative assessment. This emphasizes that effective modeling of temporal dynamics is essential for deep learning systems to interpret rehabilitation tasks and, more broadly, human action data.

27 Keypoint represents a more exploratory component of the ablation study rather than direct evidence for our claims.

Because the definition of “important” landmarks in the human body can be subjective, it was necessary to evaluate whether our custom skeleton design for the upper extremities, derived from COCO WholeBody, was appropriate for the collected data. Moreover, increasing the number of keypoints does not necessarily yield better data representation. Prior studies have noted that not all joints are equally informative and that redundant joints can introduce noise [48], [49]. Attention mechanisms have been applied to emphasize key joints within the overall context, showing that selective focus is more effective than uniform treatment. In the case of hands, which are densely articulated, excessive keypoints may even degrade performance. For instance, [50] employed graph reduction in skeleton-based sign language recognition, reporting a drop in accuracy to 63.69 when redundant nodes were removed. Since our dataset includes ADL tasks involving fine-grained hand movements, we compared model performance across skeleton configurations using our proposed 27 keypoint upper-limb representation. While larger numbers of keypoints theoretically provide more information, the results show only marginal gains for MAD and RMSE, while MAPE worsened. This implies that although absolute error magnitudes may decrease, relative accuracy compared to action scale diminishes, reflecting errors at the global contextual level. These findings suggest that for high-dimensional sequential motion data, reducing complexity while maintaining structural consistency is more effective than indiscriminately increasing keypoints.

Unlike other approaches [16]–[20], [22] that score actions by comparing input with reference movements, our method focuses on learning the mapping between action patterns and scores from training data. As shown in the Stroke-only ablation study (Table VI), training on Stroke only data produced error rates comparable to the Proposal(Table V). Because both training and testing were conducted on Stroke data, direct error metrics such as MAD observed even better results. In contrast, RMSE and MAPE exhibited higher errors than those obtained with mixed ND-Stroke data, indicating that ND sequences are more effective for capturing movement flow, whereas Stroke patient data tend to include more abrupt movements.

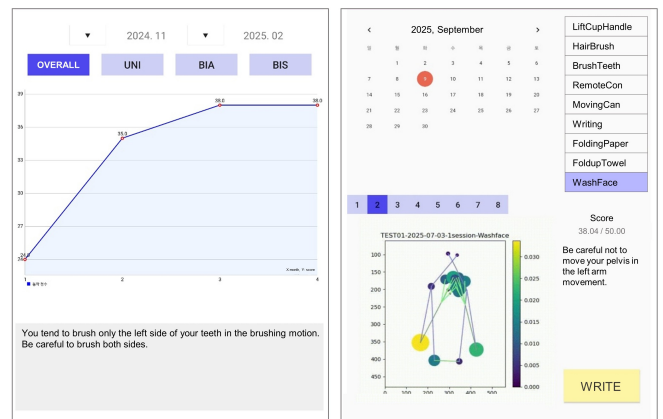


Fig. 6. Feedback from our application, Period feedback offers graph during Exercise periods(left), discrete feedback shows skeleton Graph heatmap, Score and comment each per exercise.(right)

Conclusionally the RAST-G@ with optimized frame construction (via frame dropping), temporal attention, and a 25 keypoint skeleton, preserved low MAD and RMSE while significantly reducing MAPE. This demonstrates that the model not only controls absolute error but also achieves higher relative accuracy with respect to actual motion magnitude, which is critical for rehabilitation assessment and broader human action understanding.

### C. Feedback for User

In proposing a domiciliary rehabilitation system, we also considered the need for user-friendly feedback. Model outputs must be interpretable not only to clinicians but also to patients and elderly users who may have limited familiarity with artificial intelligence, computer systems, or medical terminology. Building on the framework, our system includes a mobile application that provides comprehensive user feedback (Fig. 6). The feedback is organized into two main components: period feedback and discrete feedback.

Period feedback summarizes performance trends over time. A representative score, calculated as the average, is reported for each month to visualize changes in rehabilitation progress. The duration can be adjusted according to user preference, and performance graphs are available for overall scores as well as for specific categories such as OVERALL, UNI, BIA, and BIS. Since difficulty varies across movement categories, this enables more fine-grained evaluation. Such longitudinal feedback can assist therapists in designing and adjusting treatment plans for individual patients.

Discrete feedback records the outcome of each exercise, including skeleton heatmap visualizations, task-specific scores, and—optionally—therapist comments. This provides patients with intuitive and interpretable results, while also allowing clinicians to document and track qualitative aspects of performance. Fig. 7. illustrates the video feedback interface of our rehabilitation system. The results, derived from the assessment module including RAST-G@, highlight the most influential joints and edges in the motion sequence  $m$  at frame  $t_1$ . These are represented as heatmaps overlaid on the skeleton sequence, where color intensity and node size indicate their relative contribution to the assessment. The input tensor  $X \in \mathbb{R}^{N \times C \times T \times V \times 1}$  passes through the ST-GCN blocks to capture skeletal structure (spatial direction) along with limited temporal information, which forms the core learning representation while preserving the skeleton configuration. The resulting feature representation,  $X^L \in \mathbb{R}^{(N \times M) \times 256 \times (T/4) \times V}$  is used to generate skeleton heatmaps for visual feedback. For interpretability, the model score was rescaled to a 0–100 scale. In beta testing with physiotherapists, the system was positively received, particularly for its ability to visualize postural alignment and joint utilization. Beyond enhancing user-friendliness, the visual feedback also provides an important means to observe and analyze how the model attends to different body regions during learning.

## VI. CONCLUSION

Our approach offers the advantage of providing assessment scores without requiring a control group of healthy refer-

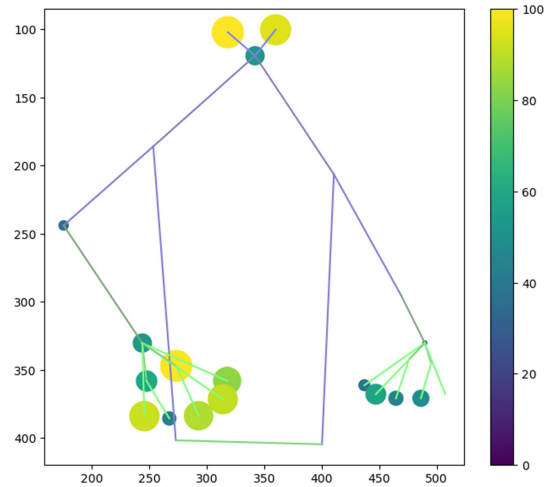


Fig. 7. Feedback with Skeleton Graph heatmap. Subject Stroke13, Label07: folding paper.

ence motions. Collecting rehabilitation movement datasets is costly regardless of whether the subjects are able-bodied or impaired. Moreover, as discussed earlier, rehabilitation assessment is conducted in terms of achieving functional activity and participation. Thus, the significance of our method lies in performing patient-centered evaluation, focusing on actual patient movements and analyzing their performance without the need for non-patient reference data. Nevertheless, the present model remains limited to assessment and does not define or prescribe recovery strategies within a comprehensive home-based rehabilitation system. Future research will focus on developing an integrated higher-level framework capable of generating recovery plans, based on more advanced analyses of individual rehabilitation exercises.

## ACKNOWLEDGMENT

This study was supported by the Translational Research Center for Rehabilitation Robots (#NRCTR-EX23008), National Rehabilitation Center, Ministry of Health and Welfare, Korea. and the Gachon University research fund of 2023(GCU-202300710001).

## REFERENCES

- [1] J. W. Krakauer, “Motor learning: its relevance to stroke recovery and neurorehabilitation;” *Current Opinion in Neurology*, vol. 19, no. 1, pp. 84–90, Feb. 2006.
- [2] V. S. Huang and J. W. Krakauer, “Robotic neurorehabilitation: a computational motor learning perspective;” *Journal of NeuroEngineering and Rehabilitation*, vol. 6, no. 1, p. 5, Dec. 2009.
- [3] M. Maier, B. R. Ballester, and P. F. M. J. Verschure, “Principles of Neurorehabilitation After Stroke Based on Motor Learning and Brain Plasticity Mechanisms;” *Frontiers in Systems Neuroscience*, vol. 13, p. 74, Dec. 2019.
- [4] K. A. Leech, R. T. Roemmich, J. Gordon, D. S. Reisman, and K. M. Cherry-Allen, “Updates in Motor Learning: Implications for Physical Therapist Practice and Education;” *Physical Therapy*, vol. 102, no. 1, p. pzb250, Jan. 2022.
- [5] Y. Hidaka, C. E. Han, S. L. Wolf, C. J. Winstein, and N. Schweighofer, “Use It and Improve It or Lose It: Interactions between Arm Function and Use in Humans Post-stroke;” *PLoS Computational Biology*, vol. 8, no. 2, p. e1002343, Feb. 2012.

- [6] K. Chen, D. Zhang, L. Yao, B. Guo, Z. Yu, and Y. Liu, "Deep Learning for Sensor-based Human Activity Recognition: Overview, Challenges, and Opportunities," *ACM Computing Surveys*, vol. 54, no. 4, pp. 1–40, May 2022.
- [7] Y. Yin, L. Xie, Z. Jiang, F. Xiao, J. Cao, and S. Lu, "A Systematic Review of Human Activity Recognition Based on Mobile Devices: Overview, Progress and Trends," *IEEE Communications Surveys & Tutorials*, vol. 26, no. 2, pp. 890–929, 2024.
- [8] M. Panwar, D. Biswas, H. Bajaj, M. Jobges, R. Turk, K. Maharatna, and A. Acharyya, "Rehab-Net: Deep Learning Framework for Arm Movement Classification Using Wearable Sensors for Stroke Rehabilitation," *IEEE Transactions on Biomedical Engineering*, vol. 66, no. 11, pp. 3026–3037, Nov. 2019.
- [9] B. Pogorelec, Z. Bosnić, and M. Gams, "Automatic recognition of gait-related health problems in the elderly using machine learning," *Multimedia Tools and Applications*, vol. 58, no. 2, pp. 333–354, May 2012.
- [10] S. Simon, J. Meining, L. Laurendi, T. Berkefeld, J. Dully, C. Dindorf, and M. Fröhlich, "2D Pose Estimation vs. Inertial Measurement Unit-Based Motion Capture in Ergonomics: Assessing Postural Risk in Dental Assistants," *Bioengineering*, vol. 12, no. 4, p. 403, Apr. 2025.
- [11] L. Xia, C.-C. Chen, and J. K. Aggarwal, "View invariant human action recognition using histograms of 3D joints," in *2012 IEEE Computer Society Conference on Computer Vision and Pattern Recognition Workshops*. Providence, RI, USA: IEEE, Jun. 2012, pp. 20–27.
- [12] H.-G. Chi, M. H. Ha, S. Chi, S. W. Lee, Q. Huang, and K. Ramani, "InfoGCN: Representation Learning for Human Skeleton-based Action Recognition," in *2022 IEEE/CVF Conference on Computer Vision and Pattern Recognition (CVPR)*. New Orleans, LA, USA: IEEE, Jun. 2022, pp. 20 154–20 164.
- [13] S. Yan, Y. Xiong, and D. Lin, "Spatial Temporal Graph Convolutional Networks for Skeleton-Based Action Recognition," Jan. 2018, arXiv: 1801.07455.
- [14] L. Xiang and Z. Wang, "Joint Mixing Data Augmentation for Skeleton-Based Action Recognition," *ACM Transactions on Multimedia Computing, Communications, and Applications*, vol. 21, no. 4, pp. 1–24, Apr. 2025.
- [15] H. Duan, Y. Zhao, K. Chen, D. Lin, and B. Dai, "Revisiting Skeleton-based Action Recognition," Apr. 2021, arXiv: 2104.13586.
- [16] R. Houmanfar, M. Karg, and D. Kulic, "Movement Analysis of Rehabilitation Exercises: Distance Metrics for Measuring Patient Progress," *IEEE Systems Journal*, vol. 10, no. 3, pp. 1014–1025, Sep. 2016.
- [17] C.-J. Su, C.-Y. Chiang, and J.-Y. Huang, "Kinect-enabled home-based rehabilitation system using Dynamic Time Warping and fuzzy logic," *Applied Soft Computing*, vol. 22, pp. 652–666, Sep. 2014.
- [18] Z. Zhang, Q. Fang, and X. Gu, "Objective Assessment of Upper Limb Mobility for Post-stroke Rehabilitation," *IEEE Transactions on Biomedical Engineering*, pp. 1–1, 2015.
- [19] D. Antón, A. Goñi, and A. Illarramendi, "Exercise Recognition for Kinect-based Telerehabilitation," *Methods of Information in Medicine*, vol. 54, pp. 145–155, Jan. 2018, publisher: Schattauer GmbH.
- [20] H. Sakoe and S. Chiba, "Dynamic programming algorithm optimization for spoken word recognition," *IEEE Transactions on Acoustics, Speech, and Signal Processing*, vol. 26, no. 1, pp. 43–49, Feb. 1978.
- [21] M. Capecchi, M. G. Ceravolo, F. Ferracuti, S. Iarlori, V. Kyrki, A. Monteriù, L. Romeo, and F. Verdini, "A Hidden Semi-Markov Model based approach for rehabilitation exercise assessment," *Journal of Biomedical Informatics*, vol. 78, pp. 1–11, Feb. 2018.
- [22] M. H. Lee, D. P. Siewiorek, A. Smailagic, A. Bernardino, and S. B. I. Badia, "Learning to assess the quality of stroke rehabilitation exercises," in *Proceedings of the 24th International Conference on Intelligent User Interfaces*. Marina del Rey California: ACM, Mar. 2019, pp. 218–228.
- [23] Y. Liao, A. Vakanski, and M. Xian, "A Deep Learning Framework for Assessing Physical Rehabilitation Exercises," *IEEE Transactions on Neural Systems and Rehabilitation Engineering*, vol. 28, no. 2, pp. 468–477, Feb. 2020.
- [24] C. Du, S. Graham, C. Depp, and T. Nguyen, "Assessing Physical Rehabilitation Exercises using Graph Convolutional Network with Self-supervised regularization," in *2021 43rd Annual International Conference of the IEEE Engineering in Medicine & Biology Society (EMBC)*. Mexico: IEEE, Nov. 2021, pp. 281–285.
- [25] Y. Mourchid and R. Slama, "MR-STGN: Multi-Residual Spatio Temporal Graph Network Using Attention Fusion for Patient Action Assessment," in *2023 IEEE 25th International Workshop on Multimedia Signal Processing (MMSP)*, Sep. 2023, pp. 1–6, arXiv:2312.13509 [cs].
- [26] S. Deb, M. F. Islam, S. Rahman, and S. Rahman, "Graph Convolutional Networks for Assessment of Physical Rehabilitation Exercises," *IEEE Transactions on Neural Systems and Rehabilitation Engineering*, vol. 30, pp. 410–419, 2022.
- [27] Y. Kong, Z. Wang, Y. Nie, T. Zhou, S. Zohren, Y. Liang, P. Sun, and Q. Wen, "Unlocking the Power of LSTM for Long Term Time Series Forecasting."
- [28] F. Kratzert, M. Gauch, D. Klotz, and G. Nearing, "HESS Opinions: Never train a Long Short-Term Memory (LSTM) network on a single basin," *Hydrology and Earth System Sciences*, vol. 28, no. 17, pp. 4187–4201, Sep. 2024.
- [29] Y. Oh, S.-A. Choi, Y. Shin, Y. Jeong, J. Lim, and S. Kim, "Investigating Activity Recognition for Hemiparetic Stroke Patients Using Wearable Sensors: A Deep Learning Approach with Data Augmentation," *Sensors*, vol. 24, no. 1, p. 210, Dec. 2023.
- [30] Z. Cao, G. Hidalgo, T. Simon, S.-E. Wei, and Y. Sheikh, "OpenPose: Realtime Multi-Person 2D Pose Estimation Using Part Affinity Fields," *IEEE Transactions on Pattern Analysis and Machine Intelligence*, vol. 43, no. 1, pp. 172–186, Jan. 2021.
- [31] L. Xu, S. Jin, W. Liu, C. Qian, W. Ouyang, P. Luo, and X. Wang, "ZoomNAS: Searching for Whole-body Human Pose Estimation in the Wild," *IEEE Transactions on Pattern Analysis and Machine Intelligence*, pp. 1–18, 2022.
- [32] A. Vakanski, H.-p. Jun, D. Paul, and R. Baker, "A Data Set of Human Body Movements for Physical Rehabilitation Exercises," *Data*, vol. 3, no. 1, p. 2, Jan. 2018.
- [33] G. Birke, S. Wolf, T. Ingwersen, C. Bartling, G. Bender, A. Meyer, A. Nolte, K. Ottes, O. Pade, M. Peller, J. Steinmetz, C. Gerloff, and G. Thomalla, "Protocol for a multicenter observational prospective study of functional recovery from stroke beyond inpatient rehabilitation - The Interdisciplinary Platform for Rehabilitation Research and Innovative Care of Stroke Patients (IMPROVE)," *Neurological Research and Practice*, vol. 2, no. 1, p. 10, Dec. 2020.
- [34] J. Lexell and C. Brogårdh, "The use of ICF in the neurorehabilitation process," *NeuroRehabilitation*, vol. 36, no. 1, pp. 5–9, Feb. 2015.
- [35] M. Capecchi, M. G. Ceravolo, F. Ferracuti, S. Iarlori, A. Monteriù, L. Romeo, and F. Verdini, "The KIMORE Dataset: KInematic Assessment of MOvement and Clinical Scores for Remote Monitoring of Physical REhabilitation," *IEEE Transactions on Neural Systems and Rehabilitation Engineering*, vol. 27, no. 7, pp. 1436–1448, Jul. 2019.
- [36] A. de Santana Correia and E. L. Colombini, "Attention, please! A survey of neural attention models in deep learning," *Artificial Intelligence Review*, vol. 55, no. 8, pp. 6037–6124, Dec. 2022.
- [37] A. Vaswani, N. Shazeer, N. Parmar, J. Uszkoreit, L. Jones, A. N. Gomez, Ł. Kaiser, and I. Polosukhin, "Attention is All you Need," *Neural Information Processing Systems (NeurIPS)*, vol. 30, 2017.
- [38] H. S. Jørgensen, H. Nakayama, H. O. Raaschou, J. Vive-Larsen, M. Støjer, and T. S. Olsen, "Outcome and time course of recovery in stroke. part ii: Time course of recovery. the copenhagen stroke study," *Archives of Physical Medicine and Rehabilitation*, vol. 76, no. 5, pp. 406–412, 1995.
- [39] OpenMMLab. (2020-2021) Mmpose: Openmmlab pose estimation toolbox and benchmark. <https://mmpose.readthedocs.io/>. Accessed: 2025-09-15.
- [40] F. Zhang, X. Zhu, H. Dai, M. Ye, and C. Zhu, "Distribution-Aware Coordinate Representation for Human Pose Estimation," in *2020 IEEE/CVF Conference on Computer Vision and Pattern Recognition (CVPR)*. Seattle, WA, USA: IEEE, Jun. 2020, pp. 7091–7100.
- [41] K. Sun, B. Xiao, D. Liu, and J. Wang, "Deep High-Resolution Representation Learning for Human Pose Estimation," in *2019 IEEE/CVF Conference on Computer Vision and Pattern Recognition (CVPR)*. Long Beach, CA, USA: IEEE, Jun. 2019, pp. 5686–5696.
- [42] Z. Kuang, J. Wang, D. Sun, J. Zhao, L. Shi, and Y. Zhu, "Hierarchical Contrastive Representation for Accurate Evaluation of Rehabilitation Exercises via Multi-View Skeletal Representations," *IEEE Transactions on Neural Systems and Rehabilitation Engineering*, vol. 33, pp. 201–211, 2025.
- [43] Y.-F. Song, Z. Zhang, C. Shan, and L. Wang, "Richly Activated Graph Convolutional Network for Robust Skeleton-Based Action Recognition," *IEEE Transactions on Circuits and Systems for Video Technology*, vol. 31, no. 5, pp. 1915–1925, May 2021.
- [44] C. Li, Q. Zhong, D. Xie, and S. Pu, "Co-occurrence Feature Learning from Skeleton Data for Action Recognition and Detection with Hierarchical Aggregation," Apr. 2018, arXiv:1804.06055 [cs].
- [45] P. Zhang, C. Lan, W. Zeng, J. Xing, J. Xue, and N. Zheng, "Semantics-Guided Neural Networks for Efficient Skeleton-Based Human Action Recognition," in *2020 IEEE/CVF Conference on Computer Vision and Pattern Recognition (CVPR)*. Seattle, WA, USA: IEEE, Jun. 2020, pp. 1109–1118.

- [46] Yong Du, W. Wang, and L. Wang, "Hierarchical recurrent neural network for skeleton based action recognition," in *2015 IEEE Conference on Computer Vision and Pattern Recognition (CVPR)*. Boston, MA, USA: IEEE, Jun. 2015, pp. 1110–1118.
- [47] S. Sardari, S. Sharifzadeh, A. Daneshkhah, S. W. Loke, V. Palade, M. J. Duncan, and B. Nakisa, "LightPRA: A Lightweight Temporal Convolutional Network for Automatic Physical Rehabilitation Exercise Assessment," *Computers in Biology and Medicine*, vol. 173, p. 108382, May 2024.
- [48] J. Liu, G. Wang, L.-Y. Duan, K. Abdiyeva, and A. C. Kot, "Skeleton-Based Human Action Recognition With Global Context-Aware Attention LSTM Networks," *IEEE Transactions on Image Processing*, vol. 27, no. 4, pp. 1586–1599, Apr. 2018.
- [49] Y. Yang, J. Zhang, J. Zhang, and Z. Tu, "Expressive Keypoints for Skeleton-based Action Recognition via Skeleton Transformation," Jun. 2024, arXiv:2406.18011 [cs].
- [50] S. Jiang, B. Sun, L. Wang, Y. Bai, K. Li, and Y. Fu, "Skeleton Aware Multi-modal Sign Language Recognition," in *2021 IEEE/CVF Conference on Computer Vision and Pattern Recognition Workshops (CVPRW)*. Nashville, TN, USA: IEEE, Jun. 2021, pp. 3408–3418.